Medical Engineering & Physics 31 (2009) 1118–1133

Contents lists available at ScienceDirect

Medical Engineering & Physics

journal homepage: www.elsevier.com/locate/medengphy

A computer model of the artificially ventilated human respiratory system in adult intensive care

A.J. Wilson[a,e], C.M. Murphy[b,f], B.S. Brook[c,e], D. Breen[d], A.W. Miles[b], D.G. Tilley[b,*]

[a] Department of Physics, University of Warwick, Coventry CV4 7AL, UK
[b] Department of Mechanical Engineering, University of Bath, Claverton Down, Bath BA2 7AY, UK
[c] School of Mathematical Sciences, University of Nottingham, Nottingham NG7 2RD, UK
[d] Department of Anaesthetics, Royal Hallamshire Hospital, Sheffield S10 2JF, UK
[e] Formerly at Department of Medical Physics and Clinical Engineering, University of Sheffield, Royal Hallamshire Hospital, Sheffield S10 2JF, UK
[f] Now at Motorola Ltd., Swindon SN25 4XY, UK

ARTICLE INFO

Article history:
Received 1 August 2008
Received in revised form 27 April 2009
Accepted 11 July 2009

Keywords:
Respiratory system
Intensive care
Mathematical modelling
Computer simulation
Lung damage

ABSTRACT

A multi-technique approach to modelling artificially ventilated patients on the adult general intensive care unit (ICU) is proposed. Compartmental modelling techniques were used to describe the mechanical ventilator and the flexible hoses that connect it to the patient. 3D CFD techniques were used to model flow in the major airways and a Windkessel style balloon model was used to model the mechanical properties of the lungs. A multi-compartment model of the lung based on bifurcating tree structures representing the conducting airways and pulmonary circulation allowed lung disease to be modelled in terms of altered $\dot{V}/\dot{Q}$ ratios within a lognormal distribution of values and it is from these that gas exchange was determined. A compartmental modelling tool, Bath*fp*, was used to integrate the different modelling techniques into a single model. The values of key parameters in the model could be obtained from measurements on patients in an ICU whilst a sensitivity analysis showed that the model was insensitive to the value of other parameters within it. Measured and modelled values for arterial blood gases and airflow parameters are compared for 46 ventilator settings obtained from 6 ventilator dependent patients. The results show correlation coefficients of 0.88 and 0.85 for the arterial partial pressures of the O_2 and CO_2, respectively ($p < 0.01$) and of 0.99 and 0.96 for upper airway pressure and tidal volume, respectively ($p < 0.01$). The difference between measured and modelled values was large in physiological terms, suggesting that some optimisation of the model is required.

1. Introduction

Modelling the human respiratory system [1–7] and in particular modelling patients undergoing artificial ventilation [8–11] have been research areas for many years. From an engineering perspective, mechanistic (compartmental) models of the respiratory system [5,6,11] appear attractive as they model anatomical structures and physiological processes in terms of easily understood engineering components. However, such an approach has a number of disadvantages: firstly, it produces models with a large number of parameters which have no direct anatomical or physiological meaning (e.g. [5,6]) and which are thus not easily understood by the physiological or clinical communities; secondly, it does not lend itself to modelling disease processes; and finally, it produces parameters which cannot be directly measured. Many mechanistic models use simple rigid tubes to describe the conducting airways, whereas in practice the conducting airways are a complex bifurcating tree structure for which many workers have proposed models [12–14]. Recent advances in 3D medical imaging and improvements in computer processing speed have allowed the geometry of the airways from individual subjects to be determined and the characteristics of air flow through them predicted using computational fluid dynamics (CFD) techniques [15,16]. We have previously demonstrated the need for 3D CFD modelling of the gas flow through the upper airways of artificially ventilated patients where Reynolds numbers in the endotracheal (ET) tube and trachea indicate turbulent and transitional flows, respectively [17].

Models of varying complexity have been proposed to describe gas exchange in the normal lung [18–21], in respiratory disease [22–26] and during artificial ventilation [27]. Much of this work utilises the theory and results obtained from the Multiple Inert Gas Elimination Technique (MIGET) [28] in which parameter estimation techniques are used with experimental data to estimate the distribution of ventilation to perfusion ($\dot{V}/\dot{Q}$) ratios based on an assumption that $\dot{V}/\dot{Q}$ ratios are lognormally distributed in a normal

* Corresponding author. Tel.: +44 01225 383023.
E-mail address: d.g.tilley@bath.ac.uk (D.G. Tilley).

1350-4533/$ – see front matter © 2009 IPEM. Published by Elsevier Ltd. All rights reserved.
doi:10.1016/j.medengphy.2009.07.009

lung. We have previously reported the development of theoretical multi-compartment models for lung disease based on bifurcating tree structures to represent the conducting airways and pulmonary circulation [29]. In models of normal lungs these bifurcating tree structures generate lognormal distributions of ventilation and perfusion in their terminal branches [29,30]. Therefore the ventilation and perfusion values from which gas exchange can be calculated can be represented by two lognormal data series. Lung disease in the bifurcating tree model is modelled by restricting flow to one or more branches of the tree which reduces the flow available for gas exchange; a process which is equivalent to reducing the numerical values of a subset of the elements in a lognormal data series [29].

Whilst the VentSim model utilised both quantitative and qualitative modelling techniques [8], the majority of models of the respiratory system to date have utilised a single modelling technique. However, the complexity of anatomical structures and physiological processes in the respiratory system suggest that this will not necessarily produce appropriate models. In this paper we describe a model of an artificially ventilated patient which incorporates four different modelling techniques: compartmental modelling for the mechanical ventilator and breathing circuit; a 3D CFD model for gas flow through the ET tube and upper airways; the bifurcating tree models we have previously described for the lower conducting airways and lung disease [29]; and non-linear algebraic models for the chemical reactions in gas exchange. One of the problems with using models of anatomical structures and physiological processes in the research or clinical environment (e.g. the VentPlan system for clinical decision support [31]) is parameter estimation. In developing the model described in this paper we focussed attention on identifying elements of the model where parameter values can be obtained by measurement on patients in the adult general intensive care unit.

The implementation of the model was based on the Bath*fp* compartmental modelling system which uses graphical icons to represent system components and which has previously been successfully used to implement a compartmental model of the breathing apparatus and human body in manned diving operations [5,6]. The open architecture of the Bath*fp* system allowed the 3D and bifurcating tree components of the model to be separately implemented and then integrated as compartments.

2. Modelling an artificially ventilated patient

2.1. Model description

Fig. 1 shows the various components (compartments) of the circuit modelled and the way in which these interconnect. The focus of the model implemented was ventilator dependant patients with acute respiratory distress syndrome (ARDS) and the ICU from which the validation data was obtained (Section 4.1) used the Dräger Evita 2 ventilator in biphasic positive airways pressure (BIPAP) mode for such patients. In this mode, the clinician controls the airway pressure during each breath by adjusting the:

(i) maximum pressure during inspiration (P_{MAX});
(ii) positive end expiratory pressure (PEEP);
(iii) time taken for the pressure to rise from PEEP to P_{MAX} (t_{ramp});
(iv) ratio between the inspiration and expiratory times (T_i:T_e);
(v) respiratory rate (RR);
(vi) fractional concentration of oxygen in the inspired gas ($F_{i_{O_2}}$).

The Evita 2 ventilator is fitted with an inspiratory valve that controls the gas flow delivered to the patient and an expiratory valve, the PEEP valve, which controls the pressure in the breathing circuit. During inspiration in the BIPAP mode the ventilator controls the opening of the inspiratory valve allowing gas to flow into the breathing circuit so that the pressure within the circuit linearly increases from PEEP to P_{MAX} in a period t_{ramp}. Once P_{MAX} is reached this pressure is maintained for the remainder of the inspiratory period, Ti. During expiration, the PEEP valve vents gas from the breathing circuit and the pressure within the circuit falls exponentially with a time constant dependant on the compliance of the lung and the resistance of the expiratory pathway through the airways, breathing circuit and ventilator until the minimum end expiratory pressure (PEEP) pressure is reached.

The model of the breathing circuit was based on a conventional arrangement where the output from the ventilator is connected via corrugated tubing to a humidifier and thence through one arm of a 'Y' piece to an ET tube where a gas tight seal with the trachea is achieved by inflating a balloon which encircles the ET tube. Expiratory gases also pass through the ET tube and are taken back to the ventilator through a corrugated tube connected to the other arm of the 'Y' piece. In terms of the model, the ventilator, corrugated tubing, humidifier, 'Y' piece and the ET tube above the seal in the trachea all form compartments within the model and were implemented using conventional mechanistic modelling techniques using equations that describe the dynamic properties of the ventilator (Section 2.2.1) and the pressure flow relationship of the gas flowing through the various circuit components (Sections 2.2.2, 2.2.3 and 2.2.6). The data exchanged between model components is the composition, temperature and mass flow rates of the gas.

Within the model the portion of the ET tube below the tracheal seal and the upper airways down to the ends of the first branches forms a single compartment. The pressure drop across this compartment determines the flow rate of air into and out of the lungs where gas exchange takes place between the alveolar gas and the blood in the pulmonary capillaries. Gas flow through this compartment was modelled using a 3D computational fluid dynamics (CFD) model as Reynolds numbers in the ET tube and airways suggest flow is turbulent and transitional, respectively [17]. The 3D model, which was implemented in CFX5.4 (AEA Technology Ltd.), was used to predict the gas flow from the end of each of the first branches in the airway given the pressures in the endotracheal tube and at the ends of the two airway branches. In order to demonstrate the principle of the approach a 3D model was implemented using typical dimensions for the trachea (diameter 25 mm) and ET tube (diameter 8 mm) and which incorporated the semi-rigid cartilaginous rings around the internal circumference of the trachea which help keep the airways open (Fig. 2). The results obtained from the CFD analysis can be included in the overall simulation model by either: (i) running CFX and Bath*fp* in parallel with data being exchanged between the two systems at each time-step or (ii) incorporating the steady state results obtained from the CFD analysis into the overall model using a lookup table which relates gas flow rate to pressure drop. Tests undertaken using the CFD model showed that following a step change in pressure, the steady state flow rate was established in less than 0.05 s and that a time-step considerably smaller than 0.001 s would be required for CFX to accurately predict the fast acting transient. As this would lead to excessive simulation run-times and the settling time was much less than the inspiratory or expiratory period, it was decided to use the lookup table approach. This was implemented by undertaking CFD simulations to determine the steady state relationship between pressure and flow rate over a physiologically realistic range of pressure and flow conditions. A typical result obtained from this analysis is shown in Fig. 3.

The mechanical properties of the left and right lungs are modelled as two elastic balloons (based on Windkessel models used to model the flow in arteries) where the gas flow rate into the lung is related to the rate of change in the pressure difference across it via the compliance of the lung and chest wall. Within the model a

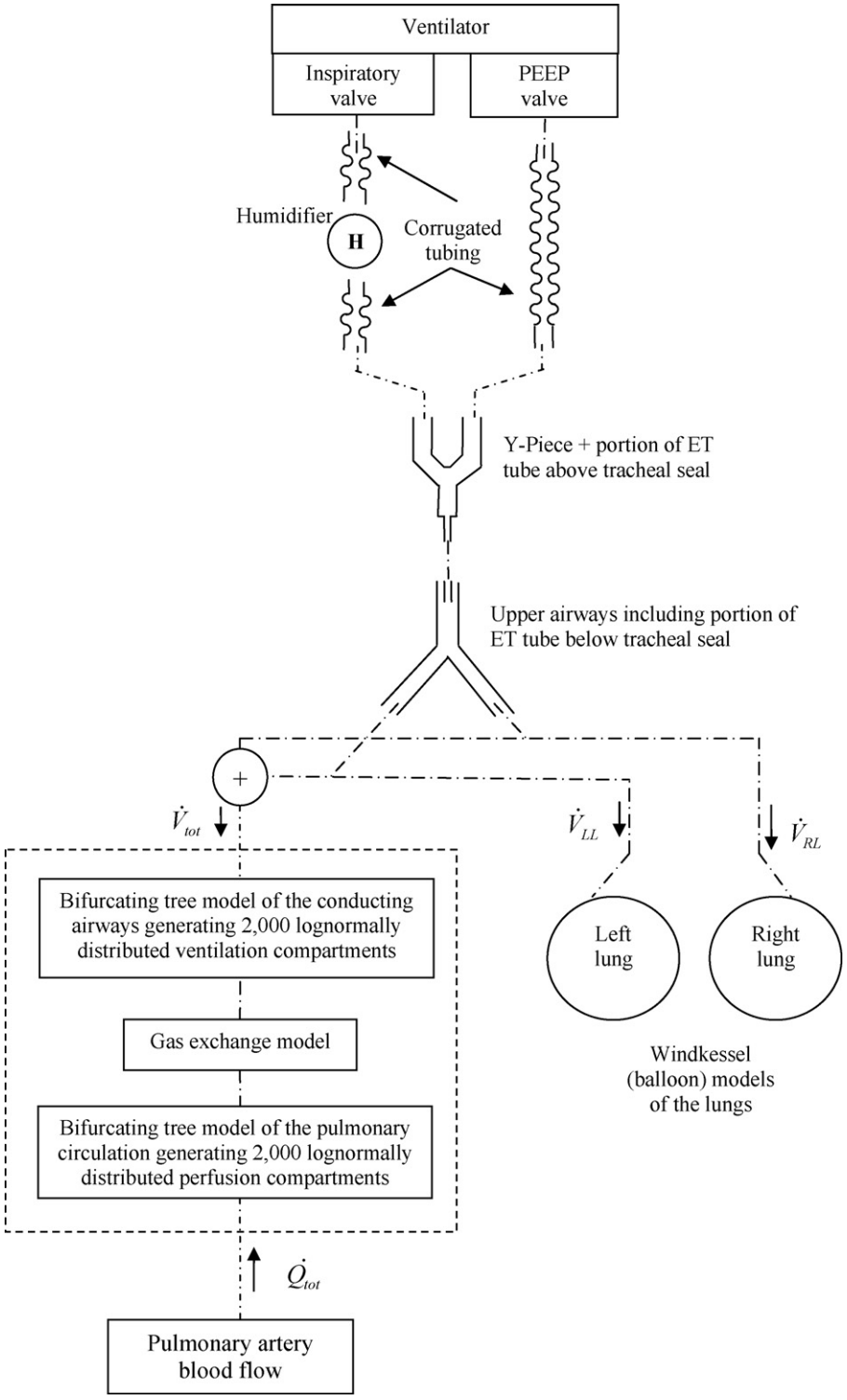

Fig. 1. Schematic diagram of the model showing the components (compartments) contained within it. The connection between model components is shown as chained lines. The portion of the model enclosed in the dashed square – identified as the functional lung model – was used to determine the lung damage.

single value is used to represent the combined compliance of the chest wall and lung and this was assumed to be independent of lung expansion rate and without hysteresis. Expansion of a lung is not the result of expansion of a single compartment, but rather the expansion of the many million individual alveoli within it. The gas exchange contribution from an individual alveoli is given by the ratio of the ventilation ($\dot{V}$) to it to the blood flow through the capillaries surrounding it ($\dot{Q}$) and a lognormal distribution of $\dot{V}/\dot{Q}$ ratios across the whole lung is commonly used to give a wide dynamic ratio of $\dot{V}/\dot{Q}$ values without generating negative values that are physiologically impossible [32,33]. To model the gas flow through the alveolar space we used a random number generator to generate 2000 lognormally distributed values which were then scaled so that the sum of the resultant data series was equal to the average flow through the 3D model during inspiration. To model the blood flow through the pulmonary capillary circulation, the random number

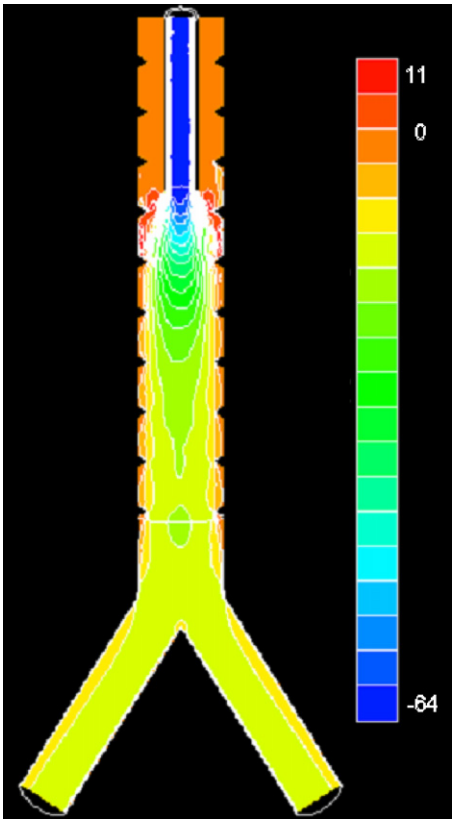

Fig. 2. A typical velocity plot from the 3D CFD analysis. The figures against the colour scale to the right hand side of the plot are in ms^{-1}.

generator was used to generate a second data series of 2000 log-normally distributed values which were scaled so that the sum of the values was equal to the average pulmonary blood flow. These uncorrelated series were then divided to a give a 2000 element series of lognormally distributed $\dot{V}/\dot{Q}$ values [29]. Studies using the Multiple Inert Gas Elimination Technique (MIGET) [28] have shown that the parameter recovery algorithms which produce lognormal distributions of $\dot{V}/\dot{Q}$ ratios for normal subjects produce bimodal distributions for subjects with lung disease [34]. Lung disease, irrespective of its aetiology, will change the distribution of $\dot{V}/\dot{Q}$ ratios. To simulate lung disease in the model we used the approach we have previously described of reducing a selected fraction of the ventilation compartments to less than 15% of their initial value which generated the bimodal distributions [29] seen in acute lung disease [35,36]. In the model we created *D*% lung damage by reducing a randomly selected *D*% of the compartments to less than 1% of their initial value so that the lung damage more closely approximates the *D*% required. Following implementation of lung damage on the ventilation data series gas exchange between the 2000 ventilation

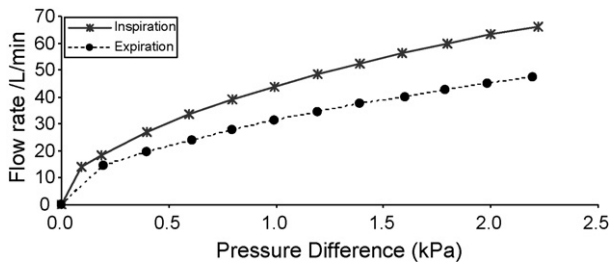

Fig. 3. 3D computational fluid dynamics analysis of pressure/flow rate relationship for the upper airways with a symmetrical bifurcation.

and perfusion compartments was calculated and the resultant values combined using mixing theory to give arterial and end tidal gas concentrations (Section 2.2.5). This calculation was performed once for each breath at the end of inspiration.

The pulmonary circulation was modelled as a compliant tube through which the blood flow was assumed to be non-pulsatile. The average blood flow thorough the pulmonary circulation was determined by the pressure drop between the right ventricle (measured as the mean pulmonary artery pressure) and left atrium (measured as the pulmonary capillary wedge pressure) and the pulmonary vascular resistance (PVR).

2.2. Mathematical analysis of model components

2.2.1. Modelling the artificial ventilator

In BIPAP mode, the pressure created by the ventilator consists of three distinct phases: inspiratory ramp, inspiratory plateau and expiration. If t_{cb} is the time into the current breath then in the inspiratory ramp phase ($0 \le t_{cb} < t_{ramp}$) the pressure generated by the ventilator to deliver gas to the breathing circuit, P_d, increases linearly as follows:

$$P_d = \text{PEEP} + \frac{t_{cb}}{t_{ramp}}(P_{MAX} - \text{PEEP}) \tag{2.1}$$

where P_d = pressure generated by the ventilator (Pa_{abs}), PEEP = positive end expiratory pressure (Pa_{abs}), P_{MAX} = maximum inspiratory pressure set on the ventilator (Pa_{abs}), t_{cb} = time into the current breath (s), and t_{ramp} = inspiratory ramp time set on the ventilator (s).

Once P_{MAX} is reached (at $t_{cb} = t_{ramp}$), the inspiratory plateau phase is entered where the pressure is held at P_{MAX} until the end of inspiration (when $t_{cb} = t_i$). When $t_{cb} > t_i$ the expiratory phase is entered and the pressure in the breathing circuit falls exponentially with a time constant that is determined by the compliance of the lung and the resistance of the airways and expiratory path through the breathing circuit and ventilator.

The model replicates the digital control action of the microprocessor controlled ventilator by sampling and updating the inspiratory valve flow rate for each sampling period. For each period, the rate of change of the mass flow rate through the inspiratory valve is determined from the difference between the generated pressure (P_d) and the inspiratory valve outlet pressure (P_{insp}):

$$\ddot{m}_{insp} = \frac{A(P_d - P_{insp})}{\Delta t}\frac{P_{insp}}{R_{in}T_{insp}} \tag{2.2}$$

where $\ddot{m}_{insp}$ = rate of change of mass flow rate through the inspiratory valve (kg/s s), P_d = generated pressure (Pa_{abs}), P_{insp} = pressure at the inspiratory valve (Pa_{abs}), A = gain term (L/s Pa), Δt = sampling period (s), T_{insp} = gas temperature at the inspiratory valve (K), and R_{in} = instantaneous gas constant (J/kg K).

A, the gain term, has been empirically determined for the Evita 2 ventilator and the instantaneous gas constant R_{in} is determined from:

$$R_{in} = \frac{R_0}{m}\sum_{i=1}^{N}\frac{m_i}{M_i} \tag{2.3}$$

where m_i = mass of constituent gas i (kg), m = total mass of gas in the lungs $\sum_{i=1}^{N} m_i$ (kg), M_i = molecular weight of constituent gas i, and R_0 = universal gas constant (J/kg K).

The inspiratory valve mass flow rate $\dot{m}_{insp}$ is determined by numerically integrating Eq. (2.2) with respect to time. Logic is included to prevent negative flow occurring at the inspiratory valve and to limit the maximum flow rate to an appropriate value.

The PEEP valve is assumed to open when the pressure in the breathing circuit exceeds the generated pressure, P_d, by a predeter-

mined amount and close when the breathing circuit pressure falls to the generated pressure. During expiration, the generated pressure is zero (Pa_{gauge}) and hence the valve is always open. The mass flow rate of gas vented from the circuit when the valve is open is determined using the standard pneumatic orifice equation [37]:

$$\dot{m}_{PEEP} = \frac{C_q C_m A_o P_{PEEP}}{\sqrt{T_{PEEP}}} \tag{2.4}$$

where $\dot{m}_{PEEP}$ = mass flow rate through the PEEP valve (kg/s), C_q = orifice flow coefficient, C_m = mass flow parameter ($\sqrt{K}$ s/m), A_o = orifice area (m^2), P_{PEEP} = gas pressure at PEEP valve inlet (Pa_{abs}), and T_{PEEP} = gas temperature at PEEP valve inlet (K).

The value for C_m depends upon whether the flow is sonic or subsonic. This is assessed using the pressures upstream and downstream of the PEEP valve and the adiabatic index for the gas. As there is a small pressure difference acting across the valve, the flow will be subsonic [37] and in this case:

$$C_m = \sqrt{\frac{2\gamma}{R_{in}(\gamma-1)\times 10^3}\left[\left(\frac{P_{ds}}{P_{us}}\right)^{2/\gamma} - \left(\frac{P_{ds}}{P_{us}}\right)^{(\gamma+1)/\gamma}\right]} \tag{2.5}$$

where P_{us} = the upstream pressure (Pa_{abs}), P_{ds} = the downstream pressure (Pa_{abs}), γ = adiabatic index for the gas, and R_{in} = instantaneous gas constant, see Eq. (2.3) (J/kg K).

2.2.2. Modelling inspiratory gas flow

During inspiration, gas flows from the ventilator to the lungs and the partial pressure of oxygen and carbon dioxide in the inspired gas can be determined from:

$$P_{O_2}^{insp} = \frac{(P_{RL} m_{RBO_2}^{insp} + P_{LL} m_{LBO_2}^{insp}) R_0}{(m_{RB}^{insp} + m_{LB}^{insp}) M_{O_2} R_{in}} \tag{2.6}$$

$$P_{CO_2}^{insp} = \frac{(P_{RL} m_{RLCO_2}^{insp} + P_{LL} m_{LBCO_2}^{insp}) R_0}{(m_{RB}^{insp} + m_{LB}^{insp}) M_{CO_2} R_{in}} \tag{2.7}$$

where $P_{O_2}^{insp}$ = inspired oxygen partial pressure (Pa_{abs}), $P_{CO_2}^{insp}$ = inspired carbon dioxide partial pressure (Pa_{abs}), P_{LL} = pressure in the left lung (Pa_{abs}), P_{RL} = pressure in the right lung (Pa_{abs}), $m_{RBO_2}^{insp}$ = mass of O_2 from the right bronchi (kg), $m_{RBCO_2}^{insp}$ = mass of CO_2 from the right bronchi (kg), $m_{LBO_2}^{insp}$ = mass of O_2 from the left bronchi (kg), $m_{LBCO_2}^{insp}$ = mass of CO_2 from the left bronchi (kg), m_{RB}^{insp} = total mass of inspired gas from right bronchi during each breath (kg), m_{LB}^{insp} = total mass of inspired gas from left bronchi during each breath (kg), M_{O_2} = molecular weight of oxygen, M_{CO_2} = molecular weight of carbon dioxide, R_{in} = instantaneous gas constant, see Eq. (2.3) (J/kg K), and R_0 = universal gas constant (J/kg K).

The amount of oxygen in the inspired gas is usually expressed as a volumetric fraction $F_{I_{O_2}}$. However, for the purposes of the dynamic modelling it is necessary to consider mass flow rates and it is more convenient to define the fractional inspired oxygen in terms of a mass ratio, $Fm_{I_{O_2}}$:

$$Fm_{I_{O_2}} = \frac{m_{O_2}^{insp}}{m_T^{insp}} \tag{2.8}$$

where m_T^{insp} = mass of inspired oxygen (kg), $m_{O_2}^{insp}$ = total mass of inspired gas (kg).

The masses of the constituent gases are determined by first initialising their values to zero at the start of each inspiration and then numerically integrating their rates of change with respect to time. For example, the mass of inspired oxygen $m_{O_2}^{insp}$ is determined from:

$$\dot{m}_{O_2}^{insp} = \frac{\dot{V}_{RB}\, m_{RBO_2}^{insp}}{m_{RB}^{insp}} + \frac{\dot{V}_{LB}\, m_{LBO_2}^{insp}}{m_{LB}^{insp}} \tag{2.9}$$

where $\dot{V}_{RB}$ = volumetric flow rate in the right bronchi (L/s), $\dot{V}_{LB}$ = volumetric flow rate in the left bronchi (L/s), $m_{LBO_2}^{insp}$ = mass of O_2 from the left bronchi (kg), $m_{RBO_2}^{insp}$ = mass of O_2 from the right bronchi (kg), m_{LB}^{insp} = total mass of inspired gas from the left bronchi during each breath (kg), m_{RB}^{insp} = total mass of inspired gas from the right bronchi during each breath (kg), and $\dot{V}_{RB}$ and $\dot{V}_{LB}$ are obtained from the 3D models (Section 2.1).

2.2.3. Mixed gas properties in the ET tube and trachea

Within the model, the common port of the Y-piece, the ET tube and the trachea are considered to form the 'upper airways' of a ventilated patient where the inspiratory and expiratory gases are mixed. The variations in upper airway gas pressure and temperature were determined by considering the mass flow rates of gas entering (Section 2.2.1) and leaving (Section 2.2.5) the upper airways (i.e. at the ET tube and the right and left bronchi). Assuming that the gas is well mixed and that the airway volume remains constant, the rate of change of pressure in the airways can be obtained by differentiating the equation of state for an ideal gas with respect to time:

$$\dot{P}_{UA} = \frac{(\dot{m}_{UA} R_{in} T_{UA} + m_{UA} \dot{R}_{in} T_{UA} + m_{UA} R_{in} \dot{T}_{UA})}{V_{UA}} \tag{2.10}$$

where $\dot{P}_{UA}$ = rate of change of pressure in upper airways (Pa/s), m_{UA} = total mass of gas in upper airways (kg), R_{in} = instantaneous gas constant, see Eq. (2.3) (J/kg K), T_{UA} = gas temperature in upper airways (K), V_{UA} = upper airways volume (L), $\dot{m}_{UA}$ = rate of change of mass of gas in upper airways (kg/s), $\dot{R}_{in}$ = rate of change of instantaneous gas constant (J/kg K s), and $\dot{T}_{UA}$ = rate of change of gas temperature in upper airways (K/s).

$\dot{R}_{in}$, the rate of change of the instantaneous gas constant is determined from

$$\dot{R}_{in} = \sum_{i=1}^{N} \frac{(\dot{m}_i m_T - m_i \dot{m}_T)}{M_i} \tag{2.11}$$

where $\dot{m}_i$ = rate of change of mass of gas i (kg), m_i = mass of gas i (kg), $\dot{m}_T$ = rate of change of total mass of gas (kg), m_T = total mass of gas (kg), M_i = molecular weight of gas i, and N = number of constituent gases.

Neglecting heat transfer effects as the surrounding tissue is perfused with blood at 37 °C, the rate of change of gas temperature can be found by considering the flow rate and temperature of the gas entering the upper airway from:

$$\dot{T}_{UA} = \frac{1}{m_{UA}} \sum_{i=1}^{N} \dot{Q}_{UA_i} (T_{in} - T_{UA}) \tag{2.12}$$

Similarly, the total mass of gas in the trachea can be determined from:

$$\dot{m}_{UA} = \sum_{i=1}^{N} \frac{\dot{Q}_{UA_i} m_{UA_i}}{m_{UA}} \tag{2.13}$$

where m_{UA} = total mass of gas in the upper airways (kg), T_{in} = gas temperature entering upper airways (K), $\dot{m}_{UA}$ = rate of change of mass of gas in upper airways (kg/s), $\dot{Q}_{UA_i}$ = flow rate of constituent gas i entering or leaving trachea (kg/s), m_{UA_i} = mass of constituent gas i entering or leaving trachea (kg), and N = number of constituent gases.

The pressure, temperature and mass are found by numerically integrating Eqs. (2.10)–(2.13) with respect to time.

2.2.4. Modelling gas flow in the lungs

The left and right lungs are represented as individual elastic chambers (balloons) whose volumes and internal gas pressures vary with time. The pressure and volume in each lung is determined separately assuming a constant temperature of 37 °C for the gas within the lung. For the right lung, the rate of change of volume is given by

$$\dot{V}_{RL} = 10^3 \times \frac{\dot{m}_{RL} R_{in} T_{RL}}{P_{RL}} \tag{2.14}$$

where $\dot{V}_{RL}$ = rate of change of right lung volume (L/s), $\dot{m}_{RL}$ = gas mass flow rate into the right lung (kg/s), R_{in} = instantaneous gas constant, see Eq. (2.3) (J/kg K), T_{RL} = gas temperature in the right lung (K), and P_{RL} = pressure within the right lung (Pa_{abs}).

The rate of change of pressure in the right lung is determined from its rate of change of volume and the effective compliance of the lung and chest wall:

$$\dot{P}_{RL} = \frac{\dot{V}_{RL}}{C_{LCW}} \tag{2.15}$$

where $\dot{P}_{RL}$ = rate of change of gas pressure (Pa/s) and C_{LCW} = effective right lung and chest wall compliance (L/Pa).

The lung volume (V_{RL}) and gas pressure (P_{RL}) are determined by numerically integrating Eqs. (2.14) and (2.15) using the functional residual lung capacity and atmospheric pressure as the initial conditions. Using similar equations to predict the pressure (P_{LL}) and volume (V_{LL}) in the left lung allows the total lung volume (V_{Ltotal}) to be determined:

$$V_{Ltotal} = V_{RL} + V_{LL} \tag{2.16}$$

2.2.5. Modelling gas exchange in the lungs

The lungs are modelled as 2000 ventilation and perfusion compartments where the values of ventilation and perfusion assigned to the compartments are lognormally distributed. The lognormal probability density function, $f(x)$, is characterised by two parameters μ_y and σ_y:

$$f(x) = \frac{1}{x\sigma_y\sqrt{2\pi}}\ e^{-1/2[(\ln x - \mu_y)/\sigma_y]^2} \tag{2.17}$$

The mean and variance for the distribution of x can be found from:

$$\text{mean} = e^{\mu_y + (\sigma_y^2/2)} \tag{2.18}$$

$$\text{variance} = e^{(2\mu_y + \sigma_y^2)}(e^{\sigma_y^2} - 1) \tag{2.19}$$

The total ventilation to both lungs is given by summing the results obtained from Eq. (2.14) for both the left and right lungs:

$$\dot{V}_{tot} = (\dot{V}_{LL} + \dot{V}_{RL}) \tag{2.20}$$

where $\dot{V}_{tot}$ = total lung ventilation (L/s), $\dot{V}_{LL}$ = left lung ventilation (L/s), and $\dot{V}_{RL}$ = right lung ventilation (L/s).

The total perfusion $\dot{Q}_{tot}$ is determined from:

$$\dot{Q}_{tot} = \frac{P_{PAP} - P_{LAP}}{PVR} \tag{2.21}$$

where $\dot{Q}_{tot}$ = blood flow rate (L/s), P_{PAP} = mean pulmonary artery pressure (Pa), P_{LAP} = left atrial pressure (Pa), and PVR = capillary bed resistance (Pa s/L).

In order to construct a lognormal distribution for a lung divided into N equal compartments, it is assumed that the values of μ for the lognormal ventilation ($\mu_{\dot{V}}$) and perfusion ($\mu_{\dot{Q}}$) distributions can be estimated from the mean ventilation ($\bar{\dot{V}}$) and perfusion ($\bar{\dot{Q}}$) to the compartments:

$$\bar{\dot{V}} = \frac{\dot{V}_{tot}}{N} \quad \text{and} \quad \bar{\dot{Q}} = \frac{\dot{Q}_{tot}}{N} \tag{2.22}$$

In the implementation of the model described in this paper N is 2000. These mean values, together with published values for the dispersion (width, quoted as LogSD) of the distributions of ventilation and perfusion for a healthy male [33] were then used to generate lognormally distributed data series of random values representing ventilation $(\dot{V}_A)_{1,\ldots,N}$ and perfusion, $(\dot{Q})_{1,\ldots,N}$. These two data series were then divided to give a 2000 value data series of $\dot{V}/\dot{Q}$ values. As discussed in Section 2.1, a randomly selected D% of the ventilation compartments are reduced to 1% of their initial value to simulate D% lung damage.

Having created a model of the lung containing 2000 ventilation and 2000 perfusion compartments, the next stage is to determine the alveolar gas composition in each compartment of the lung. This is undertaken using the approach outlined by West and Wagner [28] based on the concept of a respiratory exchange ratio (R). Assuming that the partial pressure of CO_2 in the inspired gas is zero and that no nitrogen enters or leaves the lung unit, the respiratory exchange ratios can be determined for the gas and blood as follows:

$$R_{gas} = \frac{P_{A_{CO_2}}(1 - F_{I_{O_2}})}{P_{I_{O_2}} - P_{A_{O_2}} - P_{A_{CO_2}} F_{I_{O_2}}} \tag{2.23}$$

$$R_{blood} = \frac{C_{V_{CO_2}} - C_{a_{CO_2}}}{C_{a_{O_2}} - C_{V_{O_2}}} \tag{2.24}$$

where R_{gas} = gas respiratory exchange ratio, R_{blood} = blood respiratory exchange ratio, $P_{I_{O_2}} = O_2$ partial pressure in inspired gas (Pa), $P_{A_{O_2}} = O_2$ partial pressure in alveolar gas (Pa), $P_{A_{CO_2}} = CO_2$ partial pressure in alveolar gas (Pa), $C_{V_{O_2}} = O_2$ content in mixed venous gas (L/L), $C_{V_{CO_2}} = CO_2$ content in mixed venous gas (L/L), $C_{a_{O_2}} = O_2$ content in arterial blood (L/L), and $C_{a_{CO_2}} = CO_2$ content in arterial blood (L/L).

As the gas content in the blood depends on the partial pressures of O_2 and CO_2 (see Appendix A), both Eqs. (2.23) and (2.24) are functions of the alveolar pressures. A solution for these pressures can be found by setting R_{gas} and R_{blood} equal to R, and varying R between a lower and an upper bound in steps of ΔR (termed the granularity).

The lower bound on R is determined when $P_{A_{O_2}}$ is equal to the partial pressure of O_2 in the mixed venous gas ($P_{V_{O_2}}$) and $P_{A_{CO_2}}$ is equal to the partial pressure of CO_2 in the mixed venous gas ($P_{V_{CO_2}}$), giving

$$R_{\min} = \frac{P_{V_{CO_2}}(1 - F_{I_{O_2}})}{P_{I_{O_2}} - P_{V_{O_2}} - P_{V_{CO_2}} F_{I_{O_2}}} \tag{2.25}$$

The upper bound is determined when $P_{A_{O_2}} = P_{I_{O_2}}$ and $P_{V_{CO_2}} = 0$:

$$R_{\max} = \frac{C_{V_{CO_2}}}{C_{I_{O_2}} - C_{V_{O_2}}} \tag{2.26}$$

Initial values for the gas parameters are determined using an estimate for $P_{A_{CO_2}}$ based on:

$$P_{A_{CO_2}} = \frac{R(P_{I_{O_2}} - P_{A_{O_2}})}{1 + F_{I_{O_2}}(R - 1)} \tag{2.27}$$

where $P_{I_{O_2}} = 95 \times F_{I_{O_2}}$ kPa allowing for the water content of the inspired air. Values for $P_{A_{O_2}}$ and $P_{A_{CO_2}}$ are then determined by vary-

ing $P_{A_{O_2}}$ until the following equation is satisfied:

$$R - \frac{C_{V_{CO_2}} - C_{a_{CO_2}}}{C_{a_{O_2}} - C_{V_{O_2}}} = 0 \tag{2.28}$$

The initial search interval used for $P_{A_{O_s}}$ was set between values slightly above $P_{V_{O_2}}$ (lower) and $P_{I_{O_2}}$ (upper). Iterations were continued until the residual obtained from Eq. (2.28) was less than 10^{-6}. At this point, the corresponding $\dot{V}/\dot{Q}$ ratio can be determined from:

$$\frac{\dot{V}_A}{\dot{Q}} = 8.63\,R\frac{C_{A_{O_2}} - C_{V_{O_2}}}{P_{A_{CO_2}}} \tag{2.29}$$

The values obtained for $P_{A_{O_2}}$, $P_{A_{CO_2}}$ and the $\dot{V}/\dot{Q}$ ratio are tabulated against R for values of R from R_{min} to R_{max}.

These tabulated data are then used to determine the values of $P_{A_{O_2}}$ and $P_{A_{CO_2}}$ occurring in each lung unit. This is undertaken by interpolating the tabulated $\dot{V}/\dot{Q}$ ratios for each of the $\dot{V}/\dot{Q}$ ratios in the 2000 compartment lung model. If the value of $\dot{V}/\dot{Q}$ is less than the minimum tabulated value, it is assumed that there is no ventilation occurring in that unit and the alveolar pressures are set to the mixed venous pressures. Similarly, if the value of $\dot{V}/\dot{Q}$ exceeds the maximum tabulated value then it is assumed that there is no perfusion and the pressures are set to the inspired partial pressures of O_2 and CO_2.

Having determined the post-gas exchange partial pressures for all of the lung units, the partial pressures of O_2 and CO_2 in the arterial blood and in the end tidal gases must be determined. By assuming that the alveolar and blood gas concentrations reach equilibrium at the end of gas exchange, the arterial blood gas concentrations can be obtained using the perfusion weighted mean of the alveolar gas concentrations in the individual lung compartments as follows:

$$C_{a_{O_2}} = \frac{\sum_{i=1}^{N} C_{A_{O_2},i}\dot{Q}_i}{\sum_{i=1}^{N}\dot{Q}_i} \quad \text{and} \quad C_{a_{CO_2}} = \frac{\sum_{i=1}^{N} C_{A_{CO_2},i}\dot{Q}_i}{\sum_{i=1}^{N}\dot{Q}_i} \tag{2.30}$$

where $\sum_{i=1}^{N}\dot{Q}_i = \dot{Q}_{tot}$.

Having obtained the concentrations in Eq. (2.30), the partial pressures of O_2 and CO_2 in the arterial blood can then be calculated using the oxyhaemoglobin and CO_2 dissociation equations in Appendix A. The end tidal gas concentrations are obtained using a similar approach but based on a ventilation weighted mean of the alveolar concentrations of O_2 ($C_{A_{O_2}}$) and CO_2 ($C_{A_{CO_2}}$):

$$C_{et_{O_2}} = \frac{\sum_{i=1}^{N} C_{A_{O_2},i}\dot{V}_i}{\sum_{i=1}^{N}\dot{V}_i} \quad \text{and} \quad C_{et_{CO_2}} = \frac{\sum_{i=1}^{N} C_{A_{CO_2},i}\dot{V}_i}{\sum_{i=1}^{N}\dot{V}_i} \tag{2.31}$$

where $\sum_{i=1}^{N}\dot{V}_i = \dot{V}_{tot}$.

The relationship between the end tidal gas concentrations and the partial pressures of gases in the arterial blood as a function of lung damage is shown in Fig. 4.

2.2.6. Modelling expiratory gas flow

The gas exchange is assumed to be an instantaneous process that occurs at the end of inspiration and that the gas parameters apply to both the left and right lungs. This allows the mass of the expired gases passing to the right and left bronchi to be determined using the end tidal O_2 and CO_2 partial pressures. For the right lung, the gases are determined from:

$$m^{\exp}_{RLO_2} = \frac{P^{et}_{O_2} M_{O_2} V_{RL}}{R_O T^{\exp}} \tag{2.32}$$

$$m^{\exp}_{RLCO_2} = \frac{P^{et}_{CO_2} M_{CO_2} V_{RL}}{R_O T^{\exp}} \tag{2.33}$$

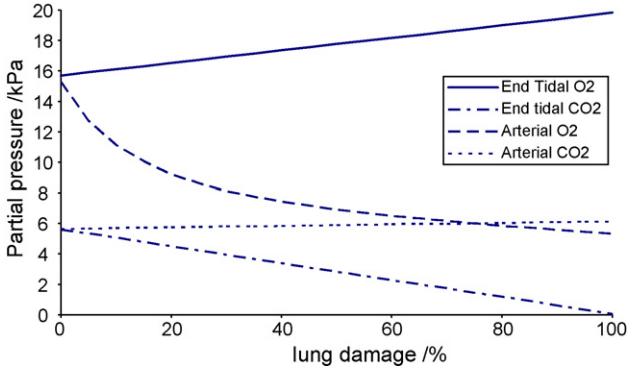

Fig. 4. The relationship between end tidal gas concentrations and arterial blood gas concentrations as a function of lung damage for the gas exchange model where the inspired gas is air and the venous blood gas concentrations for O_2 and CO_2 are 5.33 kPa and 6.13 kPa, respectively. Where there is no lung damage it can be seen that the end tidal gas concentrations approximates the alveolar gas concentration which in turn is equal to the arterial gas concentration.

$$m^{\exp}_{RLN_2} = \frac{(P_{RL} - (P^{et}_{O_2} + P^{et}_{CO_2}))M_{N_2} V_{RL}}{R_O T^{\exp}} \tag{2.34}$$

where $P^{et}_{O_2}$ = end tidal O_2 partial pressure (Pa), $P^{et}_{CO_2}$ = end tidal CO_2 partial pressure (Pa), $m^{\exp}_{RLO_2}$ = mass of O_2 expired from right lung (kg), $m^{\exp}_{RLCO_2}$ = mass of CO_2 expired from right lung (kg), $m^{\exp}_{RLN_2}$ = mass of N_2 expired from right lung (kg), $T^{\exp}$ = temperature of expired gas (K), R_0 = universal gas constant (J/kg K), M_{O_2}, M_{CO_2}, M_{N_2} = O_2, and CO_2 and N_2 molecular weights.

2.3. Example simulations

To illustrate the performance of the model example simulations were run using the parameter values given in Table 1. Fig. 5 shows the variation in predicted lung volume and the O_2 and CO_2 partial pressures within the breathing circuit at PEEP settings of 0

Table 1
Parametric data used for the example simulations.

Ventilator
Inspiration ramp time = 0.5 s
Gas temperature = 20 °C
Breaths/min = 10
Inspiratory:expiratory ratio = 0.5
Interconnecting hoses
Internal diameter = 10 mm
Length = 1 m
Y-piece
Internal volume = 100 mL
Humidifier
Internal volume = 1 L
Lungs
Functional residual capacity = 2 L
Total lung and chest wall compliance = 440 mL/kPa
Temperature of gas in lung = 37 °C
Ventilation distribution dispersion = 0.35 (mL/m)^2
Perfusion distribution dispersion = 0.43 (mL/m)^2
Haemoglobin = 10 g/dL
Blood temperature = 37.5 °C
Haematocrit saturation fraction = 0.44
Blood pH 7.26
Capillary bed resistance = 0.11 kPa s/mL
Pulmonary pressure differential = 1.33 kPa
Mixed venous O_2 partial pressure = 5.33 kPa
Mixed venous CO_2 partial pressure = 6.13 kPa
Number of lung units = 2000

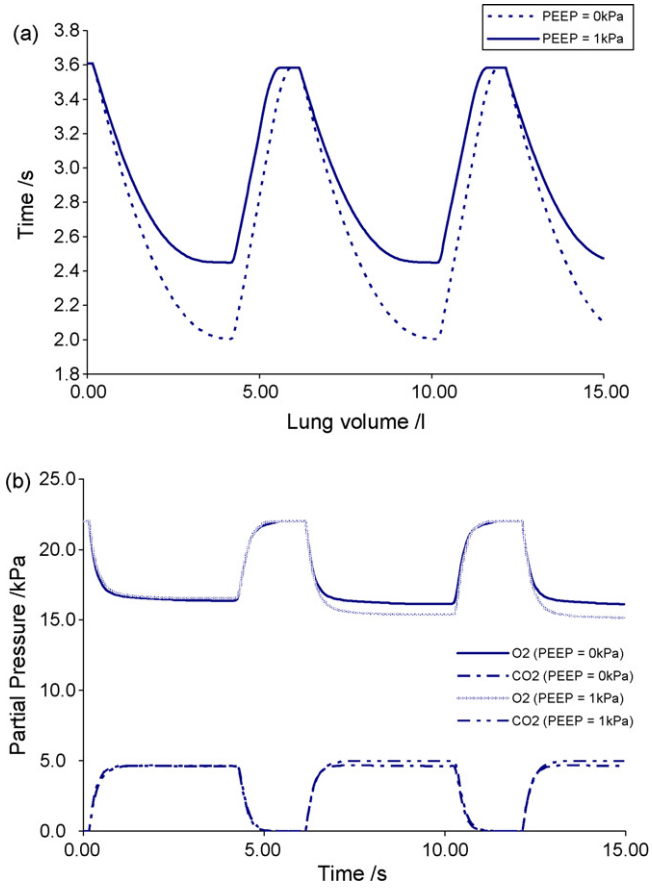

Fig. 5. Variation in predicted lung volume and the O_2 and CO_2 partial pressures in the trachea for a healthy lung at PEEP settings of 0 and 1 kPa. The ventilator was set at 10 breaths/min, $F_{i_{O_2}} = 21\%$ and the inspiratory pressure = 3.5 kPa. All other settings are given in Table 1.

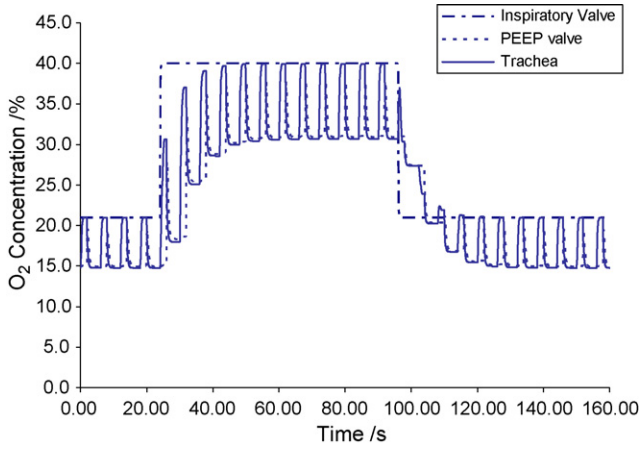

Fig. 6. Variation in oxygen concentration at the ventilator mixer valve outlet, PEEP valve inlet and in the trachea with ventilator O_2 setting. O_2 concentration increased from 21% to 40% at 24 s and reduced back to 21% at 96 s. PEEP was set to 1 kPa and Pinsp to 3.5 kPa.

and 1 kPa. At zero PEEP, the lung volume increases from its functional residual capacity (FRC) of 2 L to 3.6 L as the pressure from the ventilator linearly increases from atomospheric pressure to the maximum inspiratory pressure which was set to 3.5 kPa. The lung volume remains at 3.6 L until the PEEP valve opens allowing gas to vent from the circuit returning the lung volume to 2 L. A PEEP pressure of 1.0 kPa increases the FRC to 2.44 L, which reduces the tidal volume from 1.6 L to 1.16 L for the same maximum inspiratory pressure.

Fig. 6 shows the effect of changing the fraction of O_2 in the inspired gas from 21% to 40%. The plots, showing the O_2 concentrations at the mixer valve outlet, the PEEP valve inlet and the trachea for a healthy lung, demonstrate the underlying the dynamics of the respiratory model.

3. Model parameters and model sensitivity

3.1. Materials and methods

The equations used to model the physiological processes must be developed in terms of physical quantities that are conserved (e.g. mass, energy and momentum). However, clinicians and physiologists commonly use non-conserved measures such as volumetric flow rates and the partial pressure of gases in solutions to quantify variables. Within the current model we have formulated input and output variables in terms of measures commonly used within an ICU and converted these to fundamental quantities prior to processing within the model. Table 2a lists the parameters which are input to the model. These are either parameters which are set on the ventilator, directly measured from patients or which are calculated from measurements made. Of these, the only one that is problematical is the lung damage as there is currently no commonly used quantitative measure of lung disease.

Table 2a
Input parameters for respiratory model.

Measured
pH of blood
Mixed venous O_2
Mixed venous CO_2
Pulmonary artery pressure
Pulmonary capillary wedge pressure
Calculated
Compliance of lung
Resistance of the lung capillary bed
Lung damage
Set on ventilator
Inspiratory pressure
Expiratory pressure
Breath frequency
Tinsp:Texp ratio
Time for a ramp up inspiration

In addition to the information about an individual patient, the models require details of the breathing circuit including the volumes of the humidifier, ET tube, Y piece and interconnecting pipework (Table 2b). These parameters were measured once and then assumed to remain constant. To assess the sensitivity of the model to the values of these parameters the gain factor approach proposed by Sun and Beshara [38] was used. In this the sensitivity was expressed as the sensitivity gain:

$$\text{sensitivity gain} = \left| \frac{\%\ \text{change in predicted value}}{\%\ \text{change in parameter value}} \right| \quad (3.1)$$

Table 2b
Circuit parameters—parameters of the breathing circuit which were measured once and then assumed to be constants.

Circuit parameters
Volume of ET tube
Volume of Y-piece
Expiratory valve diameter
Maximum flow allowed at mixer valve
Volume of humidifier
Volume of breathing circuit pipe work

Table 2c
Assumed parameters—parameters which are not routinely measured on an ICU but which the model requires.

Assumed parameters
Gas supply temperature
Functional residual capacity
Temperature of gas flowing out of lung
Haemoglobin saturation in blood
Temperature of blood
Haematocrit fractional saturation in blood
Dispersion of ventilation distribution
Dispersion of perfusion distribution

and a model was deemed insensitive to a parameter if the sensitivity gain was less than 0.1 for a 10% change in value of that parameter. In this study the sensitivity gain was measured for the predicted values of tidal volume, airways pressure, and the arterial gas partial pressures $P_{a_{O_2}}$ and $P_{a_{CO_2}}$.

The sensitivity gain for the all parameters in Table 2b was determined by perturbing the values by +10%. In addition to the parameters which are input to the model (Table 2a) and the circuit parameters (Table 2b), there are a small number of parameters (Table 2c) where values are either rarely measured, or are difficult to measure, on the ICU. The sensitivity gains of all the parameters in Table 2c, with the exception of the two dispersion parameters, were determined for a 10% increase in value. Because of the non-linear nature of the oxyhaemoglobin dissociation curve and the presence of parameters which affect gas exchange in Table 2c (e.g. haemoglobin), the sensitivity gain for these parameters were measured at 10% lung damage and 90% lung damage. The two dispersion parameters in Table 2c determine the width of the ventilation and perfusion distributions in the multi-compartment lung model. These parameters have no effect on either the airways pressure or tidal volume, but potentially have an effect on the calculated gas exchange. Values of 0.35 and 0.43 are quoted for the dispersion of the ventilation and perfusion distributions, respectively [33]. These have been rarely measured and thus a high level of uncertainty must be attached to the published values. Therefore the sensitivity gain of the model to these parameters was determined using values obtained for $P_{a_{O_2}}$ and $P_{a_{CO_2}}$ at different values of lung damage as the variance parameters were varied between 0.1 and 1.5 in increments of 0.2.

3.2. Model parameter sensitivity results

None of the parameters in Table 2b, the parameters that were measured once and then assumed to be constant, showed a sensitivity gain greater than 0.01 and therefore the model was judged to be insensitive to the values of these parameters.

For the assumed parameters in Table 2c, the sensitivity gain for those parameters involving gas exchange, the sensitivity gain was always greater at 10% lung damage than at 90% lung damage. At 90% lung damage, only the sensitivity gain for the change in $P_{a_{O_2}}$ with haemoglobin was >0.01 and it had a value of 0.04. For 10% lung damage the results of the sensitivity analysis are given in Table 3. From this it can be seen that none of the parameters had a sensitivity gain greater than 0.1 and the majority of parameters had a sensitivity gain of less than 0.01. Therefore the model was deemed insensitive to these parameters.

Fig. 7 shows how the arterial blood gas values change with lung damage as the dispersion of the ventilation and perfusion distributions are changed. The non-linear nature of the two $P_{a_{O_2}}$ graphs originate from the non-linearity of the oxyhaemoglobin dissociation curve. The sensitivity gain for $P_{a_{CO_2}}$ was less than 0.1 for all values of dispersion and for all values of lung damage for both the ventilation and perfusion. Therefore the model prediction of $P_{a_{CO_2}}$ was deemed insensitive to the variance parameters. As can be seen from Fig. 7, changes in both the variance parameters have a similar effect on the predicted $P_{a_{O_2}}$ values with the greatest model sensitivity being at 0% lung damage. For 0% lung damage the sensitivity gain for both the dispersion parameters was less than 0.1 for dispersion values less than 0.7. This figure is much greater than the values for dispersion quoted in the literature and therefore the model predictions of $P_{a_{O_2}}$ were also deemed insensitive to the values of dispersion used.

Table 3
Sensitivity gain values for the assumed parameters (with the exception of the dispersion parameters) at 10% lung damage. Values less than 0.01 are shown in '–'.

Parameter	Tidal volume	Airways pressure	$P_{a_{O_2}}$	$P_{a_{CO_2}}$
Gas supply temperature	–	–	0.01	–
Functional residual capacity lungs	0.05	–	–	–
Temperature of gas flowing out of lung	0.03	–	–	–
Haemoglobin saturation in blood	–	–	0.07	–
Haematocrit fractional saturation in blood	–	–	–	0.02
Temperature of blood	0.03	–	–	0.02

4. Model validation

4.1. Materials and methods

To demonstrate that the parameter values for the model could be obtained from patients on an adult general ICU and to investigate the ability of the model to predict, and track changes in, key parameters used to assess the success of respiratory therapy delivered on an ICU we compared measured and model predicted values of the arterial blood gases ($P_{a_{O_2}}$ and $P_{a_{CO_2}}$), the airways pressure and the tidal volume following a change in the ventilator setting of fully ventilated patients on an adult general ICU.

Six fully ventilated patients (Draeger Evita 2, BiPAP) from the ICU at the Royal Hallamshire Hospital, Sheffield were studied (Table 4). All the patients had a primary diagnosis of acute respiratory distress syndrome and had no history of asthma or other chronic lung disorders. All patients were sedated with a standard regime of Morphine and Madezolam, were stable on the ventilator and were undergoing the standard invasive monitoring procedures for that ICU including a routinely inserted Swan-Ganz catheter for the measurement of cardiac output. The study received ethical committee approval from the South Sheffield Ethics Committee and informed consent was obtained from the relatives prior to study commencement.

In order to validate the model, haemodynamic, blood gas and respiratory data were required. A personal computer (PC) fitted with a 12-bit analogue to digital converter (adc) board (Computer Boards Ltd., DAS1601/12) running a data collection programme specifically written for the project formed the data acquisition system. Analogue signals from the bedside monitor (Kontron Supermon or Marquette 8000 series) corresponding to the continuously monitored cardiovascular parameters (arterial blood pressure (ABP), pulmonary artery pressure (PAP) and central venous pressure (CVP)) were directly input to the data acquisition system through the analogue to digital converter (adc) board sampling at 40 Hz. Pulmonary capillary wedge pressure (PCWP) and cardiac output (CO) measurements which require manual intervention were made using the bedside monitors but the values were entered into the data acquisition system manually. Arterial and venous blood gas measurements were made from blood sam-

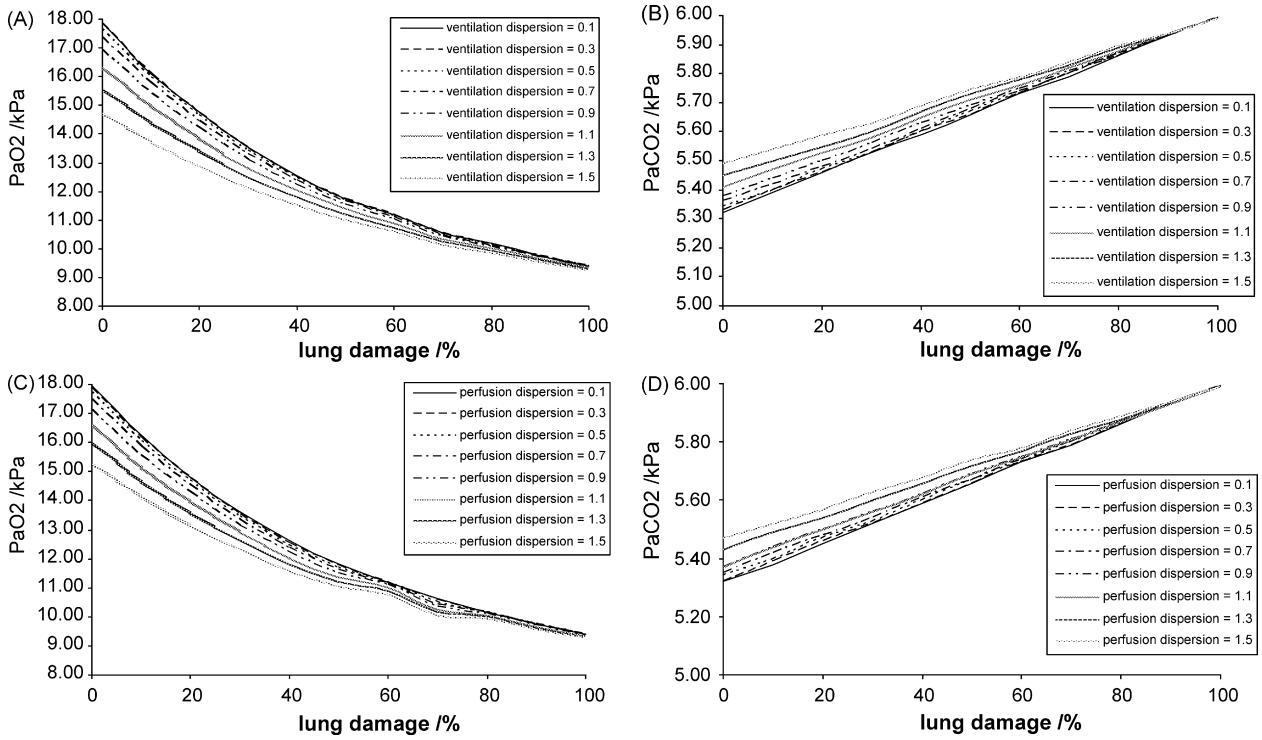

Fig. 7. (A and B) The effects of changing the ventilation dispersion parameter on the predicted values of $P_{a_{O_2}}$ and $P_{a_{CO_2}}$, respectively whilst the dispersion parameter for perfusion is held constant at 0.43. (C and D) The effects of changing the perfusion dispersion parameter on the predicted values of $P_{a_{O_2}}$ and $P_{a_{CO_2}}$, respectively whilst the dispersion parameter for ventilation is held constant at 0.35.

ples withdrawn from the patient, analysed in a laboratory area situated on the ICU and then the values manually entered into the data acquisition system. To obtain respiratory data, a pneumotachograph (Metabo type 2 coupled with a Furness Controls FCD40 pressure transducer) to measure flow, a pressure transducer (Becton–Dickinson, IDT series) to measure upper airway pressure and a gas sampling tube connected to an end tidal CO_2 ($ETCO_2$) monitor (Datex Capnomac) were placed at the top of the endotracheal tube. The pressure transducers for the pneuomatachograph, and the airways pressure measurements were connected to a set of specially designed amplifiers. The analogue outputs from these, together with the analogue output from the $ETCO_2$ monitor were connected to the adc board of the data acquisition system and the signals digitised at 40 Hz. In addition to the measures requiring manual intervention (PCWP and CO), the data acquisition system allowed the results of arterial and venous blood gas measurements and the ventilator settings to be entered manually during the study. All data, whether manually or automatically entered, were time stamped. The data acquisition system included an 'event marker' which allowed changes in ventilator setting to be identified in the data. During the study all time continuous parameters could be displayed on the screen of the data acquisition system and this, together with the number of channels sampled, limited the sampling rate to 40 Hz.

Prior to each study the transducers used for the respiratory measurements were calibrated. The calibration process was supported by the data acquisition system. After zeroing the pressure transducer, two precision rotameters calibrated for air and oxygen (Elsag Baily Ltd.) were used to calibrate the pneumotachograph at 100 L/min at the $F_{i_{O_2}}$ currently being used to treat the particular patient. The upper airways pressure transducer was calibrated against an independently calibrated Druck DPI701 digital pressure indicator.

The study was based around making changes in the ventilation regime. Four parameters were available for change: inspiratory pressure (P_{insp}), end expiratory pressure (PEEP), the ratio of inspiratory to expiratory time (T_i:T_e) and the fraction of inspired oxygen ($F_{i_{O_2}}$). The pressures could be changed in either direction by 0.5 kPa;

Table 4
Details of the patients studied together with the ventilator settings, cardio-respiratory measures and blood gas values prior to study commencement.

	Subject					
	1	2	3	4	5	6
Demographic						
Age (years)	84	36	45	74	80	61
Sex	M	F	M	F	M	M
Height (m)	1.75	1.70	1.88	1.76	1.70	1.78
Weight (kg)	80	75	110	70	70	75
Ventilator settings						
Pinsp (kPa)	2.5	3.5	2.5	2.5	2.0	2.5
PEEP (kPa)	0.7	1.0	0.8	0.5	0.5	1.5
Ramp (s)	0.5	0.5	0.5	0.5	0.5	0.5
$F_{i_{O_2}}$ (%)	40	50	40	40	35	50
Resp rate (min^{-1})	11	14	12	12	10	15
T_i:T_e	1:2	1:2	1:2	1:2	1:2	1:1
Cardiovascular						
Heart rate (bpm)	63	101	94	90	135	128
Mean ABP (kPa)	8.9	7.5	11.6	10.0	11.2	8.4
Mean PAP (kPa)	3.7	4.3	3.7	3.7	3.7	3.2
PCWP (kPa)	1.6	2.5	1.5	2.0	1.6	2.0
CVP (kPa)	1.3	2.0	1.0	1.6	0.9	1.2
Cardiac output (L/min)	6.0	4.2	10.8	8.7	11.8	10.3
Blood gas						
pH	7.28	7.43	7.25	7.32	7.21	7.18
$P_{a_{O_2}}$ (kPa)	14.2	19.4	19.8	15.6	17.2	27.8
$P_{a_{CO_2}}$ (kPa)	5.8	5.6	7.3	4.8	4.3	5.3
$P_{v_{O_2}}$ (kPa)	7.7	6.1	11.1	5.8	6.4	7.0
$P_{v_{CO_2}}$ (kPa)	6.4	7.4	7.7	4.1	5.1	6.1

allowable values of T_i:T_e were 1:2, 1:1 and 2:1 and $F_{i_{O_2}}$ could be changed by 5% in either direction.

At the start of the study and following each change in a ventilator setting, there was a 15 min measurement period throughout which the continuous variables were recorded. At the end of this period, the measurements requiring manual intervention (PCWP, CO, arterial and venous blood gases) were measured and the values manually entered into the data acquisition system. Four 15 min measurement periods were associated with each parameter of the ventilator changed and all changes started with a 15 min measurement period where the ventilator was set to the pre-study values for that patient. One of the ventilation parameters was then altered and, following a 15 min measurement period, returned to its pre-study value. After a further 15 min measurement period, the same pattern was repeated but this time the same ventilator parameter was altered in the other direction. Changes in up to 3 ventilator parameters were carried out on any one patient.

In order to make comparisons between subjects it was necessary to derive summary values for the continuously monitored variables. For systemic arterial and pulmonary arterial blood pressures, the systolic, diastolic and mean values were determined for the 10 heartbeats at the end of each 15 min measurement period. Flow data from the pneumotachograph was integrated to give volume and the average tidal volume determined for the last 10 breaths at the end of each 15 min measurement period. Similarly, the average maximum and minimum upper airway pressures and end tidal CO_2 values were determined for the last 10 breaths of each 15 min measurement period.

The pulmonary circulation is modelled as a constant flow through a tube (Eq. (2.21), Section 2.2.5). Within the model there is no interaction between the respiratory and cardiac components of the model. In order to determine whether this assumption was valid for the patients studied, changes in the heart rate, cardiac output, mean arterial blood pressure and mean pulmonary artery pressure were measured between the end of adjacent 15 min measurement periods. Because changes were not always in the same direction, differences were quantised as either 'change' or 'no change'. Pressure differences <5 mmHg, heart rate differences <10 bpm and cardiac output values <0.5 L/min were classified as 'no-change'. The probability of change was assessed by comparing these values with the differences in the same parameters classified in an identical manner between successive periods when the ventilator was set to its pre-study values. Statistical significance was assessed using a chi-squared test with a Bonferroni correction for multiple measurements.

The input parameters for the model are given in Table 2a. The parameters which are either measured or set on the ventilator require no further explanation. Of the three calculated parameters, two: the compliance of the lung and the resistance of the lung capillary bed can be obtained from the respiratory and cardiovascular measurements respectively. The lung compliance was determined from the tidal volume and the change in the upper airway pressure during inspiration (P_{insp} − PEEP) on a breath-by-breath basis and averaged over the last 10 breaths in each measurement period. An average value for each patient was then calculated and used in all the model analyses for that patient. The resistance of the lung capillary bed is taken as the pulmonary vascular resistance which is calculated according to Eq. (2.21) from measurements of the mean pulmonary artery pressure, the pulmonary capillary wedge pressure which approximates the left atrial pressure and the cardiac output.

The final calculated parameter is the % lung damage which is problematical because lung damage is not normally quantified. In order to obtain a value for this parameter the pulmonary circulation, ventilation and gas exchange models (shown within the dashed square in Fig. 1 and collectively referred to as the 'functional lung model'), were used in isolation of the rest of the model. The principal inputs to the functional lung model were the volumetric flow rates of gas and blood to the lungs, the mixed venous blood gas concentrations and the percentage lung damage from which the model calculated the arterial blood gas concentrations. With the exception of the percentage lung damage, measured values of the input parameters and the arterial blood gases are obtained before and after each change in the ventilator settings. Using these, the functional lung model was used to determine the arterial blood gas concentrations for values of lung damage between 1% and 100% at 1% intervals. These calculated values of the arterial $P_{a_{O_2}}$ and $P_{a_{CO_2}}$ were then compared to the measured values to determine the % lung damage for O_2 and CO_2 separately. This process was repeated for each ventilator setting used on a particular patient and an average value for the % lung damage was then determined for each gas for that patient. No changes were made to the perfusion compartments.

For each set of measurements taken, the parameters given in Table 2a were fed into the model. The model was then run for 12 breaths which experiments had shown produced results within 99% of those produced at 120 breaths. The measured arterial blood gas values, upper airway pressures and tidal volumes predicted were then compared against those predicted by the model. The correlation between measured and modelled values were determined using Pearson r.

4.2. Model validation results

The results from 45 ventilator settings on 6 patients are presented. This data set yielded cardiovascular measurements for 40 changes in ventilator setting (20 P_{insp}, 11 PEEP, 4 T_i:T_e, 5 $F_{i_{O_2}}$) and 18 measurements from successive periods where the ventilator was set to its pre-study values. Comparisons of changes in the mean arterial pressure, mean pulmonary artery pressure, heart rate and cardiac output between these 2 sets of measurements revealed no significant differences (Table 5). Therefore, the assumption within the model that there was no cardio-respiratory interaction as a result of the study protocol was valid for the patients studied.

Results for the determination of the % lung damage are shown in Table 6. Because of the high variability of the results and the small number of changes in ventilator settings for some patients, the results have been quoted as median and range in addition to the more common mean ± S.E.M. From the table it can be seen that the

Table 5
The results of comparing changes in cardiovascular system (CVS) measures with and without changes in ventilator settings.

CVS parameter	CVS parameter status following a change in ventilator setting		CVS parameter status for adjacent periods of identical ventilator setting		χ^2	Significance ($p < 0.05$)
	No change	Change	No change	Change		
MAP	27	13	10	8	2.15	NS
PAP	37	3	16	2	0.50	NS
HR	31	9	13	5	0.60	NS
CO	22	18	8	10	1.96	NS

Table 6
Assessment of the % lung damage for 6 subjects.

Subject	No. of measurements	%Lung damage for O_2			%Lung damage for CO_2		
		Median	Mean ± S.E.M.	Range	Median	Mean ± S.E.M.	Range
1	9	79	80 ± 3.1	67–100	28	25 ± 4.9	0–48
2	9	65	65 ± 3.8	51–77	0	0 ± 0	0–0
3	4	45	49 ± 8.3	33–72	0	27 ± 13.2	0–53
4	4	65	62 ± 8.2	39–78	75	62 ± 24.0	0–100
5	8	52	53 ± 1.5	47–59	26	35 ± 13.5	0–100
6	11	44	44 ± 0.8	40–49	0	0 ± 0	0–0

value obtained for % lung damage for oxygen and carbon dioxide are different. Since the primary purpose of artificial ventilation is to maintain adequate blood oxygenation, we have used the median % damage for oxygen in the model validation.

The results for correlating the measured and modelled arterial blood gases are shown in Figs. 8 and 9. The results for the statistical analysis give r values for arterial O_2 and CO_2 as 0.85 and 0.88, respectively, both of which are significant at $p < 0.01$. The slope of the line of best fit for the scatter plots shown in Figs. 8 and 9 are 0.66 and 0.77, respectively. This shows that the model is predicting arterial blood gas values that are lower than the measured values but that it is tracking changes in these values. In the clinical environment absolute values matter and Figs. 10 and 11 give plots of the difference between he measured and modelled values against the measured values of $P_{a_{O_2}}$ and $P_{a_{CO_2}}$ respectively. From these it can be seen that the error in the model's prediction of $P_{a_{O_2}}$ increases with the measured values whilst the error in the model's prediction of $P_{a_{CO_2}}$ is largely independent of the absolute values.

The results for the measured and modelled upper airway pressure and tidal volume are shown as scatter plots in Figs. 12 and 13. The analysis of these data gives r values for upper airway pressure and tidal volume of 0.99 and 0.96, respectively. Once again, both of these values are statistically significant at $p < 0.01$. The slope of the line of best fit for the scatter plots shown in Figs. 12 and 13 are 1.5 and 1.3, respectively. This shows that the model is predicting upper airway pressure and tidal volume values that are higher than the measured values but that it is tracking changes in these values. The errors in the model's prediction of upper airways pressure and tidal volume are shown in Figs. 14 and 15, respectively.

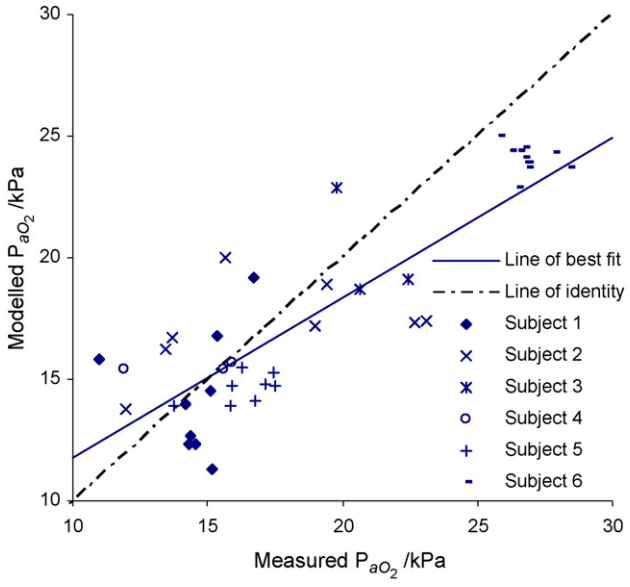

Fig. 8. The comparison of modelled $P_{a_{O_2}}$ against measured $P_{a_{O_2}}$. Both the line of best fit and the line of identity are shown.

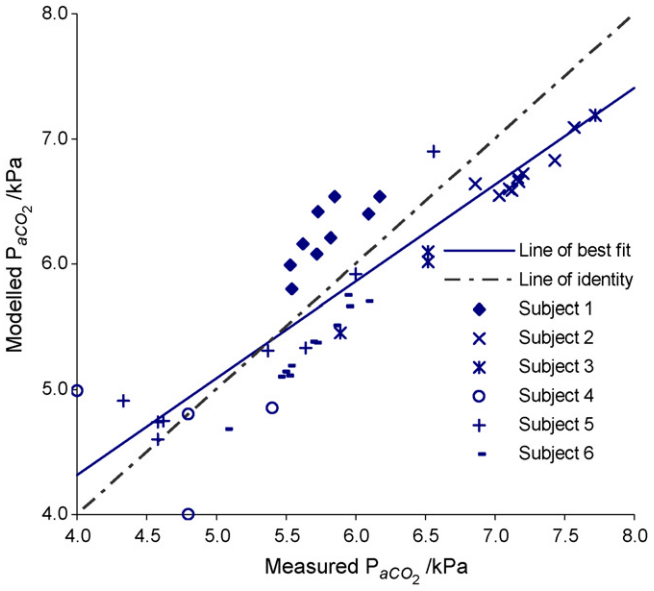

Fig. 9. The comparison of modelled $P_{a_{CO_2}}$ against measured $P_{a_{CO_2}}$. Both the line of best fit and the line of identity are shown.

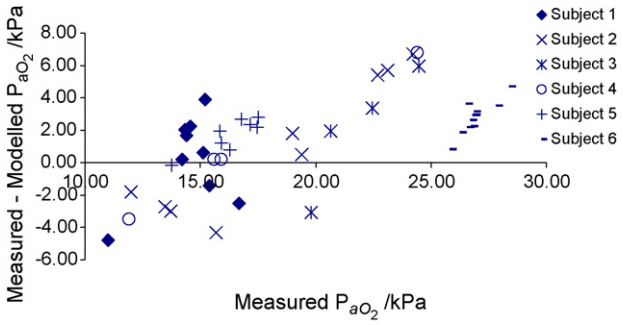

Fig. 10. A plot of the difference between the measured and modelled arterial partial pressure of oxygen against the measured arterial partial pressure of oxygen.

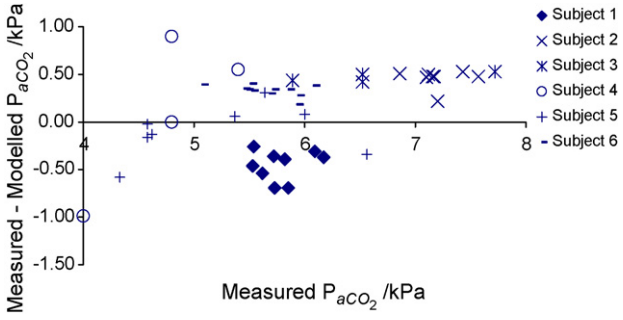

Fig. 11. A plot of the difference between the measured and modelled arterial partial pressure of carbon dioxide against the measured arterial partial pressure of carbon dioxide.

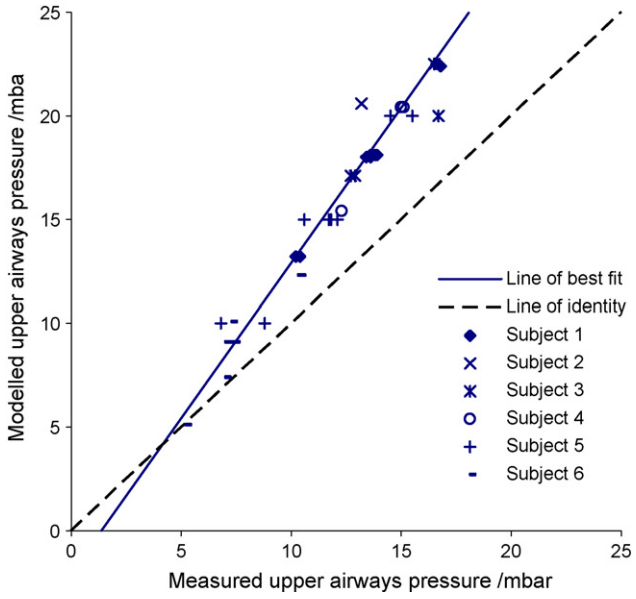

Fig. 12. The comparison of modelled upper airway pressure against measured mouth pressure. Both the line of best fit and the line of identity are shown.

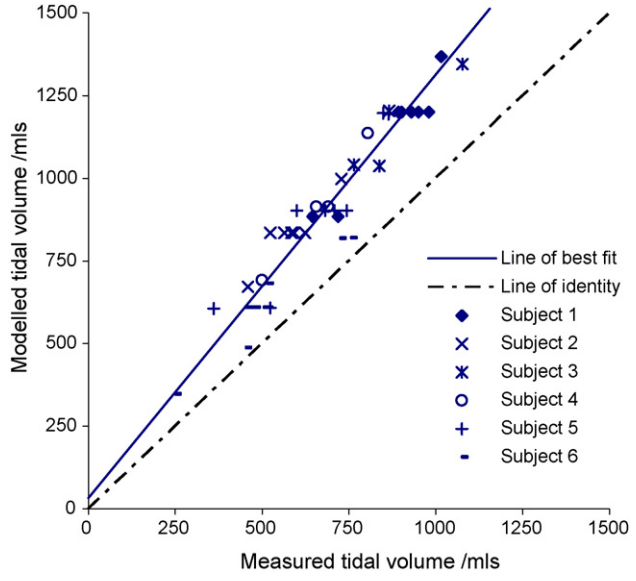

Fig. 13. The comparison of modelled tidal volume against measured tidal volume. Both the line of best fit and the line of identity are shown.

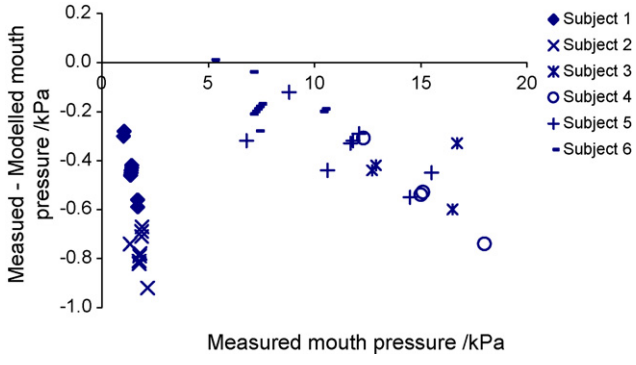

Fig. 14. A plot of the difference between the measured and modelled mouth pressure against the measured mouth pressure.

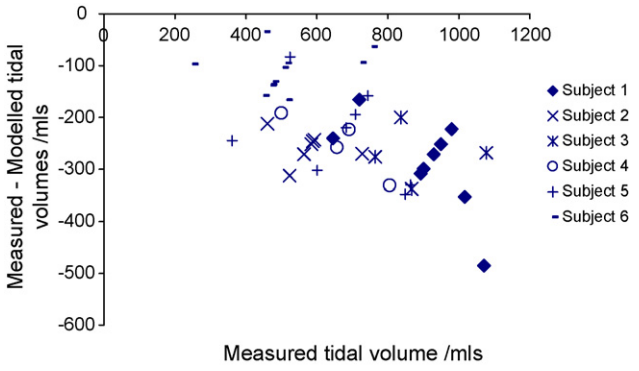

Fig. 15. A plot of the difference between the measured and modelled tidal volume against the measured tidal volume.

5. Discussion and conclusions

In this paper we have described a model of an artificially ventilated patient on an adult general ICU where a compartmental modelling tool has been used as a 'shell' to integrate compartments constructed from different modelling techniques. Our aim was to produce a model which could be parameterised for individual patients on an adult general ICU. All models contain some unknown parameters and a sensitivity analysis showed that the model was insensitive to values of these for predictions of tidal volume, airways pressure and the arterial blood gas values ($P_{a_{O_2}}$ and $P_{a_{CO_2}}$).

The single most common organ system failure for patients treated in an adult general ICU is respiratory failure where patients are unable to maintain adequate oxygenation through acute respiratory disease and require artificial ventilation. Therefore a focus of the work has been on modelling lung disease and the gas exchange in diseased lungs. The basis of our model of the lung has been to use multiple ventilation and perfusion compartments where the ventilation and perfusion values to those compartments are lognormally distributed. Lung damage is modelled by reducing the ventilation value to a randomly selected subset of those compartments to reflect disease (Section 2.1). We divided the unordered series of ventilation and perfusion values to produce the series of $\dot{V}/\dot{Q}$ values needed for the gas exchange calculations and thus assumed there was no correlation between ventilation and perfusion within the lung. It is generally accepted that in the normal lung ventilation and perfusion are correlated and that the matching between ventilation and perfusion is actively maintained [39,40]. However, when lung damage was induced in an animal model, plots of $\dot{V}$ against $\dot{Q}$ showed an increased spread around the straight line $\dot{V}/\dot{Q} = 2$ when compared with animals without lung damage [41]. Lung damage is known to be regional in ARDS [35,36] and this finding in an animal model is consistent with areas of the lung where there is either a reduced or very different correlation. We have previously shown that a $\dot{V}/\dot{Q}$ data series produced by dividing lognormal ventilation and perfusion data series is itself lognormally distributed irrespective of whether the input data series are correlated or not [29]. In this work we have adopted the precautionary strategy of not assuming that ventilation and perfusion are correlated in ARDS. Few numerical values exist for the dispersion of lognormal ventilation and perfusion distributions and MIGET cannot be used with patients on the ICU. The result from the sensitivity analysis showed that the predictions of $P_{a_{O_2}}$ and $P_{a_{CO_2}}$ were insensitive to the values of the dispersion parameters. Whilst this result is important from the perspective of the model it also requires further explanation because of the obvious changes in arterial blood gas values with dispersion value changes, particularly at low levels of lung dam-

age (Fig. 7). Lognormal distributions have been used to describe ventilation and perfusion distributions because they allow a wide dynamic range without producing negative values which are physiologically impossible. However, the theory behind the use of these distributions [28] requires the log mean of the ventilation, perfusion and ventilation to perfusion ratio distributions be close to unity and therefore the values of the dispersion parameter are small compared to the dynamic range of values. Because of the shape of the lognormal distribution, and in particular its long tail as the measure increases, the majority of values will lie around the mean value and this will result in only a small impact on the calculated blood gas values as the dispersion parameter is changed.

Much of the theory behind using ventilation–perfusion ratios to determine gas exchange is based on mixing theory with steady state flows. MIGET [28] estimates the distribution of $\dot{V}/\dot{Q}$ ratios from the measured retention and elimination of a number (typically 6) of inert gases from the pulmonary space over a number of breaths. The assumption in the parameter recovery algorithms used to process the experimental data obtained in a MIGET experiment is that there are average flows from which the $\dot{V}/\dot{Q}$ ratios are estimated. In our model, the average inspiratory flow for each breath was used to calculate the gas exchange on a breath-by-breath basis at the end of inspiration. Within the model, ventilation values are available throughout the breathing cycle and using the model equations currently implemented, it would be possible to calculate the gas exchange at discrete time points throughout each breath and track the changes in $P_{a_{O_2}}$ and $P_{a_{CO_2}}$ which occur during a breath. However, this would be computationally expensive and provide little Additional information in terms of the work we have carried out given that we could only measure blood gases at 15 min intervals when we came to obtain data from the ICU.

One of our aims was to be able to parameterise the models based on measurements made on the adult general ICU. Because mixing theory forms the basis of the $\dot{V}/\dot{Q}$ techniques for determining gas exchange, it is necessary to have both the flow through the pulmonary circulation and the mixed venous blood gas values. To obtain data for model validation we used fully ventilated patients who had a pulmonary artery catheter inserted, but the use of these is becoming increasingly less common. There are a number of devices available that either non-invasively or minimally invasively estimate cardiac output by a variety of techniques and values from these could be used to provide a value for the blood flow through the pulmonary circulation. Peripheral venous blood gases values can be obtained without difficulty and it may be possible to extend the model to predict the mixed venous values from these based on a knowledge of the metabolic state of the patient.

Lung damage is also a parameter required by the model but there is currently no method of quantifying this. Clinicians involved in the routine care of patients on the ICU primarily use a subjective assessment of the chest X-ray. A score has been proposed which uses a number of measures including qualitative assessment of X-rays and the ratio of $F_{i_{O_2}}$ to $P_{a_{O_2}}$ to assess the degree of lung injury [42]. However, this score is not widely used in either clinical medicine or research and does not yield a quantitative measure of lung damage. Therefore the functional lung model (Fig. 1) was used with the measured values of the arterial and venous blood gases to determine lung damage values for O_2 and CO_2. The large differences obtained in the values of these were not anticipated and their origins (particularly in the results for CO_2) are not obvious. One possibility lies in the nature of the lung damage: if the damage resulted from alveolar membrane thickening due to liquid absorption the larger solubility of CO_2 when compared with O_2 would potentially produce a smaller level of lung damage for CO_2 when compared with O_2. Conversely, small airways plugging restricting flow to the alveoli would be expected to produce similar levels of damage for O_2 and CO_2. The current lung model is based on mixing theory and cannot distinguish between airways plugging and an impaired alveolar membrane. Clearly, the findings require validation through further experimentation and a more complete physiological model of the respiratory system. Within the context of the current work it was decided to use % damage determined for oxygen because the primary reason that patients are artificially ventilated is because they cannot maintain adequate blood oxygenation. The assumption in taking the average value of lung damage for each patient was that the magnitude and duration of changes in the ventilator settings were not sufficient to make a significant change in the degree of lung damage. Whilst using the functional lung model to determine the lung damage has allowed validation of the current model, there is clearly a need to develop an independent measure of lung damage.

The results obtained comparing the arterial blood gas results with the measured values obtained from patients show a high level of correlation and reasonable agreement in terms of the absolute values. This indicates that the model is tracking changes in arterial O_2 and CO_2 concentrations following changes in ventilator settings. The non-unity slope of the line of best fit obtained from the data suggests that some optimisation of the models is necessary.

The modelling of the breathing circuit was implemented using conventional mechanistic modelling techniques. For the work described in this paper we have modelled the BIPAP mode of the Dräger Evita 2 as this was used to obtain the validation. However, there is no reason why the principles used for modelling this ventilator [43] could not be applied to generating models for other ventilators. In the current implementation of the model, the lung and chest wall compliance are characterised by a single value which is independent of the rate of lung expansion and around which there was no hysteresis. The complexity of the compartment could be increased to separate the lung and chest wall compliances and include the more familiar sigmoidal shaped curve of the lung compliance together with the changes in lung compliance with rate of filling. However, the former would require oesophageal pressure measurements which are not routinely made on the ICU. The simple single value used in the current implementation establishes the principle of a compartment for which numerical values can be easily obtained by direct patient measurement, but the poor agreement between the measured an modelled values for mouth pressure and tidal volume probably reflect this over-simplification. Even including hysteresis and a dynamic compliance term would be an over-simplification as a diseased lung may have many time constants in it and there is no method of measuring these on an ICU.

The use of 3D models for the ET tube and upper airways was based on an expectation of turbulent or transitional flow patterns and these were seen in the 3D analysis. However, to make this part of the model patient specific it is necessary to have cross sectional imaging data. Whilst CT and MRI scans are not routinely performed on patients within ICUs, chest X-rays are routinely performed. We have previously shown that it is possible to achieve a partial 3D reconstruction from 2D images using a model based technique [44] and a similar approach could possibly be used here. Prototype 'mini-CTs' that could be used on an ICU have already been demonstrated by the main medical equipment manufacturers so routine cross sectional imaging of ICU patients could become a reality in the not too distant future.

The results presented in this paper show that there is no significant response in the cardio-respiratory measures following a change in ventilator settings. Therefore the initial assumption that in ventilator dependent patients with a primary diagnosis of ARDS the respiratory system could be modelled independently of the cardiac system was justified. However, if the respiratory system was to be modelled as patients became less ventilator dependent and during weaning when there is less sedation

then consideration would have to be given to modelling that interaction.

Whilst the correlations between the measured and modelled values for airways pressure and tidal volume were good, the absolute differences between the two sets of values were large when considered in terms of what would be significant in patient treatment. Currently our 3D CFD model of the upper airways only extends down to the ends of the first branches. Extending this model further down the tracheo-bronchial tree will better quantify the resistance to flow in the airways and allow modelling of restrictive lung diseases. This and other improvements in the modelling of the breathing circuit and respiratory mechanics may produce improvements in the predictions obtained from the model, but this may require parameters which cannot be easily measured on the ICU. Compartmental models are inherently dynamic models but because the model we have described predicts values that can only be measured at discrete points in time (e.g. blood gases) a validation of its dynamic properties was not possible.

Acknowledgements

The authors acknowledge the financial support of the Engineering and Physical Sciences Research Council (EPSRC) through grants GR/L74323 and GR/L74835.

Appendix A.

The blood gas composition is determined using the mathematical descriptions of the oxygen and carbon dioxide dissociation curves described by West and Wagner [28]. These have been simplified to omit the Haldane effect to eliminate recursive calculation of the concentration and partial pressure values.

The oxygen content is found using:

$$C_{a_{O_2}} = 1.39\ S_a H_b + S_{O_2} P_{V_O} \tag{A1}$$

where H_b = blood haemoglobin content (g/dL), S_a = oxygen saturation of blood (%), and S_{O_2} = oxygen solubility (taken to be 0.003 mLO_2/mLblood/mmHg).

The amount of oxygen saturated in the blood depends on the level of $P_{V_{O_2}}$ and is given by

$$S_a = \frac{AP_{V_{O_2}} + BP^2_{V_{O_2}} + CP^3_{V_{O_2}} + P^4_{V_{O_2}}}{D + EP_{V_{O_2}} + FP^2_{V_{O_2}} + GP^3_{V_{O_2}} + P^4_{V_{O_2}}} \quad (\text{when } P_{V_{O_2}} \geq 10\,\text{mmHg}) \tag{A2}$$

or

$$S_a = 0.003683\,P_{V_{O_2}} + 0.000584 P^2_{V_{O_2}} \quad (\text{when } P_{V_{O_2}} < 10\,\text{mmHg}) \tag{A3}$$

where $A = -8532.2289$, $B = 2121.4010$, $C = -67.073989$, $D = 935960.87$, $E = -31346.258$, $F = 2396.1674$ and $G = -67.104406$.

The carbon dioxide content in the blood, $C_{a_{CO_2}}$ (mL/100 mL) is determined from

$$C_{a_{CO_2}} = 2.22(C^C_{CO_2} H_{crit} + C^P_{CO_2}(1 - H_{crit})) \tag{A4}$$

where $C^C_{CO_2}$ = CO_2 content in blood cells (mL/100 mL), $C^P_{CO_2}$ = CO_2 content in blood plasma (mL/100 mL), and H_{crit} = haematocrit content.

The plasma and blood cell carbon dioxide contents are determined from:

$$C^P_{CO_2} = S^P_{CO_2} P_{V_{CO_2}} (1 + 10^{(\text{pH} - pK)}) \tag{A5}$$

$$C^C_{CO_2} = D_{\text{int}} C^P_{CO_2} \tag{A6}$$

where $S^P_{CO_2}$ = CO_2 solubility coefficient (mmol/L/mmHg), pH = blood pH value, D_{int} = ratio of CO_2 in cells to that in plasma and pK is defined as

$$pK = 6.086 + 0.042(7.4 - \text{pH}) + (38.0 - T)(0.0047 + 0.0014(7.4 - pH)) \tag{A7}$$

where T is the temperature in °C.

The solubility coefficient for CO_2, $S^P_{CO_2}$, is given by

$$S^P_{CO_2} = 0.0307 + 0.00057(37.0 - T) + (0.00003(37.0 - T)^2 \tag{A8}$$

D_{int} is determined using ratios for fully oxygenated (D_{oxy}) and fully reduced blood (D_{red}) as follows:

$$D_{int} = D_{oxy} + (D_{red} - D_{oxy}) \left(1 - \frac{S_a}{100}\right) \tag{A9}$$

where

$$D_{oxy} = 0.59 + 0.21913(7.4 - \text{pH}) - 0.0844(7.4 - \text{pH})^2 \tag{A10}$$

$$D_{red} = 0.664 + 0.2275(7.4 - \text{pH}) - 0.0938(7.4 - \text{pH})^2 \tag{A11}$$

Finally, the partial pressure of CO_2 can then be found from:

$$P_{a_{CO_2}} = \frac{C_{CO_2}}{2.22\ S^P_{CO_2}(1 - H_{crit}(1 - D_{int})(1 + 10^{(\text{pH} - pK)}))} \tag{A12}$$

Conflict of interest

No benefits in any form have been received or will be received from a commercial party related directly or indirectly to the subject of this article.

References

[1] Grodins FS, Buell J, Bart J. Mathematical analysis and digital simulation of the respiratory control system. J Appl Physiol 1967;22:260–76.
[2] Dickinson CJ. A computer model of human respiration. MTP Press Ltd.; 1977.
[3] Saunders KB, Bali HN, Carson ER. A breathing model of the respiratory system: the controlled system. J Theor Biol 1980;84:135–61.
[4] Sarhan NAS, Leaning MS, Saunders KB, Carson ER. Development of a complex model: breathing and its control in man. Biol Med Meas Infro Contr 1987;2:81–100.
[5] Tomlinson SP, Lo JKW, Tilley DG. Time transient gas exchange in the respiratory system. IEEE Eng Med Biol 1993;12:64–70.
[6] Tomlinson SP, Lo JKW, Tilley DG. Computer simulation of human interaction with underwater breathing equipment. Proc Inst Mech Eng H 1994;209:249–61.
[7] Batzel JJ, Tran HT. Stability of the human respiratory control system. I. Analysis of a two-dimensional state-space model. J Math Biol 2000;41:45–79.
[8] Rutledge GW. VentSim: a simulation model of cardiopulmonary physiology. J Am Med Inform Assoc 1994;(Suppl. S):878–83.
[9] Winkler T, Krause A, Kaiser S. Simulation of mechanical respiration using a multicompartment model for ventilation mechanics and gas exchange. Int J Clin Monit 1995;12:231–9.
[10] Graham MR, Haberman CJ, Brewster JF, Girling LG, McManus BM, Mutch WAC. Mathematical modelling to centre low tidal volumes following acute lung injury: a study with biologically variable ventilation. Respir Res 2005;6 [article 64].
[11] Polak AG, Mroczka J. Nonlinear model for mechanical ventilation of human lungs. Comput Biol Med 2006;36:41–58.
[12] Pedley, Schroter RC, Sudlow MF. Energy losses and pressure drop in the models of the human airways. Respir Physiol 1970;9:371–86.
[13] Phillips CG, Kaye SR, Schroter RC. A diameter based reconstruction of the branching pattern of the human bronchial tree. Part II. Mathematical formulation. Respir Physiol 1994;98:219–26.
[14] Nithiarasu P, Hassan O, Morgan K, Weatherill NP, Fielder C, Whittet H, et al. Steady flow through a realistic human upper airway geometry. Int J Numer Methods Fluids 2008;57:631–58.
[15] Ley S, Mayer D, Brook BS, van Beek EJR, Heussel CP, Rinck D, et al. Radiological imaging as the basis for a simulation software of ventilation in the tracheobronchial tree. Eur Radiol 2002;12:2218–28.
[16] Wang J, Tetlow GA, Lucey AD, Armstrong JJ, Leigh MS, Paduch A, et al. Dynamics of the human upper airway: on the development of a three-dimensional computational model. IFMBE Proc 2007;14:3449–52.
[17] Wilson AJ, Brook BS, Murphy CM, Breen D, Miles AW, Tilley DG. Multi-modal modelling of the human respiratory system in intensive care. IFMBE Proc 2002;3:1594–5.

[18] Bellenal H, Busso T. Analysis of end-tidal and arterial PO_2 gradients using a breathing model. Eur J Appl Physiol 2000;83:402–8.
[19] Whitley JP, Gavaghan DJ, Hahn CEW. Mathematical modelling of pulmonary gas transport. J Math Biol 2003;47:79–99.
[20] Ben-Tal A. Simplified models for gas exchange in the human lungs. J Theor Biol 2006;238:474–95.
[21] Rees SE, Kjærgaard S, Andreassen S, Hedenstierna G. Reproduction of MIGET retention and excretion data using a simple model of gas exchange in lung damage caused by oleic acid infusion. J Appl Physiol 2006;101: 826–32.
[22] Benetar SR, Hewlett AM, Nunn JF. The use of iso-shunt lines for control of oxygen therapy. Br J Anaesth 1973;45:711–8.
[23] Yamaguchi K, Mori M, Kawai A, Takasugi T, Asano K, Oyamada Y, et al. Ventilation–perfusion inequality and perfusion impairment in acutely injured lungs. Respir Physiol 1994;98:165–77.
[24] Loeppky JA, Caprihan A, Altobelli SA, Icenogle MV, Scotto P, Vidal Melo MF. Validation of a two-compartment model of ventilation/perfusion distribution. Respir Physiol Neurobiol 2006;151:74–92.
[25] Yem JS, Turner MJ, Baker AB, Young IH, Crawford ABH. A tidally breathing model of ventilation, perfusion and volume in normal and diseased lungs. Br J Anaesth 2006;97:718–31.
[26] Niklason L, Eckerström J, Jonson B. The influence of venous admixture on alveolar dead space and carbon dioxide exchange in acute respiratory distress syndrome: computer modelling. Crit Care 2008;12:R53.
[27] Drummond GB, Zhong NS. Inspired oxygen and oxygen transfer during artificial ventilation for respiratory failure. Br J Anaesth 1983;55:3–13.
[28] West JB, Wagner PD. Pulmonary gas exchange. In: West JB, editor. Bioengineering aspects of the lung, 3. USA: Marcel Decker Inc.; 1977. p. 361–457.
[29] Brook BS, Murphy CM, Breen D, Miles AW, Tilley DG, Wilson AJ. Theoretical models for the quantification of lung injury using ventilation and perfusion distributions. Comput Math Methods Med 2009;10:139–54.
[30] Qian H, Bassingthwaighte JB. A class of flow bifurcation models with lognormal distribution and fractal dispersion. J Theor Biol 2000;205:261–8.
[31] Rutledge GW, Thomsen GE, Farr BR, Tovar MA, Polaschek JX, Beinlich IA, et al. The design and implementation of a ventilator-management advisor. Artif Intell Med 1993;5:67–82.
[32] Lenfant C, Okubo T. Distribution function of pulmonary blood flow and ventilation–perfusion ratio in man. J Appl Physiol 1968;24:668–77.
[33] Wagner PD, Laravuso RB, Uhl RR, West JB. Continuous distributions of ventilation–perfusion ratios in normal subjects breathing air and 100% O_2. J Clin Invest 1974;54:54–68.
[34] Dantzker DR, Brook CJ, Dehart P, Lynch JP, Weg JG. Ventilation–perfusion distributions in adult respiratory distress syndrome. Am Rev Respir Dis 1979;120:1039–52.
[35] Varon J, Wenker OC. The acute respiratory distress syndrome: myths and controversies. Internet J Emerg Intensive Care Med 1997, http://www.ispub.com/journals/IJEICM/Vol1N1/ards.htm.
[36] Luce JM. Acute lung injury and the acute respiratory distress syndrome. Crit Care Med 1998;2:369–76.
[37] Massey BS. Mechanics of fluids. 4th ed. Van Nostrand Reinhold Co.; 1979. p. 379–430.
[38] Sun Y, Beshara M, Lucariello J, Chiaramida SA. A comprehensive model of the right–left heart interaction under the influence of pericardium and baroreflex. Am Physiol Soc 1997:H1499–515.
[39] Simon BA, Tsusaki K, Venegas JG. Changes in regional lung mechanics and ventilation distribution after unilateral pulmonary artery occlusion. J Appl Physiol 1997;82:882–91.
[40] Altemeier WA, McKinney S, Glenny RW. Fractal nature of regional ventilation distribution. J Appl Physiol 2000;88:1551–7.
[41] Altemeier WA, Robertson HT, Glenny RW. Pulmonary gas-exchange analysis by using simultaneous deposition of aerosolized and injected microspheres. J Appl Physiol 1998;85:2344–51.
[42] Murray JF, Matthay MA, Luce JM, Flick MR. An expanded definition of the adult respiratory distress syndrome. Am Rev Respir Dis 1998;138:720–3.
[43] Murphy CM, Brook B, Tilley DG, Miles AW, Breen D, Wilson A. The validation of computer models of a mechanical ventilator and the human respiratory system intended for use in adult intensive care. In: Proceedings of the IMACS symposium on mathematical modelling, vol. 1. 2000. p. 251–4 [ARGESIM Report No: 15].
[44] Brook BS, Murphy CM, Breen D, Miles AW, Tilley DG, Wilson AJ. Quantification of lung injury using ventilation and perfusion distributions obtained from gamma scintigraphy. Physiol Meas 2007;28:1451–64.